Adsorption of Reactive Yellow 145 onto Chitosan Coated Magnetite Nanoparticles

Nuzhet Ayca Kalkan,[1] Serpil Aksoy,[1] Eda Ayse Aksoy,[2,3] Nesrin Hasirci[3,4,5,6]

[1]*Department of Chemistry, Faculty of Science, Gazi University, Teknikokullar, 06500 Ankara, Turkey*
[2]*Central Laboratory, Middle East Technical University, 06800 Ankara, Turkey*
[3]*BIOMATEN-Center of Excellence in Biomaterials and Tissue Engineering, METU, 06800, Ankara, Turkey*
[4]*Graduate Department of Micro&Nano Technology, Middle East Technical University, 06800 Ankara, Turkey*
[5]*Graduate Department of Biotechnology, Middle East Technical University, 06800 Ankara, Turkey*
[6]*Department of Chemistry, Faculty of Arts and Sciences, Middle East Technical University, 06800 Ankara, Turkey*

Received 10 January 2011; accepted 27 May 2011
DOI 10.1002/app.34986
Published online 5 October 2011 in Wiley Online Library (wileyonlinelibrary.com).

ABSTRACT: Removal of dyes from the industrial discharge water is an important issue for safety of the environment. In this study, magnetic (magnetite, Fe_3O_4) nanoparticles were coated with chitosan (CS) and the efficiency of these chitosan coated magnetic nanoparticles (Fe_3O_4-CS) for the adsorption of a reactive textile dye (Reactive Yellow 145, RY145) was examined first time in literature. TEM, XRD, and EPR results revealed that the thickness of the coat was about 2–5 nm, no phase change in the spinel structure of magnetic particles existed after coating, and particles had paramagnetic property, respectively. Adsorption of RY145 on Fe_3O_4-CS nanoparticles occurs according to Langmuir model in the temperature range 25°C–45°C with a maximum adsorption capacity of 47.62 mg g^{-1} at 25°C, in aqueous media. Thermodynamic parameters demonstrated that the adsorption process was endothermic and spontaneous, and the maximum desorption of the dye was 80% over a single adsorption/desorption cycle. In this study, the high efficiency of the CS coated magnetic nanoparticles in the adsorption and removal of reactive dyes from water was shown on model RY145. This type of nanoparticles can be good candidates in industrial applications for the decolorization of waste waters. © 2011 Wiley Periodicals, Inc. J Appl Polym Sci 124: 576–584, 2012

Key words: magnetic nanoparticles; chitosan; TEM; EPR; adsorption

INTRODUCTION

Dyes are widely used in various industries including cosmetic, plastic, paper, food, and textile industries. Their presence in the discharge water is hazardous since they threat the ecosystem, damage the aquatic life, and create problems for human health. Therefore, there is an intense research going on to explore new techniques and sorbent materials to remove the dyes from the waste water. In fact, this is not an easy process since most of the dyes are recalcitrant organic molecules, resistant to aerobic digestion, and are stable to light, heat, and oxidizing agents.[1,2] In some cases the dye itself might not be so resistant but the organic chemicals which are formed by degradation or oxidation of the dye can be recalcitrant to atmospheric conditions.[3] Although there are several physical, chemical, biological, acoustical, radiational, and electrical processes for the removal of the dyes, adsorption is the most preferable physical process because of its simplicity and high efficiency. In adsorption process, the dye is collected and concentrated on the surface of a solid material which can be easily removed from its medium.[4] The solid adsorbent can be regenerated and be used many times for the same purpose. To remove the dyes from aqueous media, different adsorbents including alumina,[5] silica gels,[6] zeolites,[7] activated carbon,[8] etc., have been used. However, investigations related to development of novel effective and economical adsorbents are still in progress. In the recent years, magnetic micro and nanoparticles have been widely studied for removal of dyes and pollutants from the wastewaters. Use of magnetic micro and nano adsorbents have some advantages such as having large specific surface area effective for adsorption, ease of separation from the adsorption medium by magnetic separation, and having no internal diffusion resistance in the adsorption media.[9–11] Coating of the magnetic adsorbents with polymers containing functional groups or ions increases their adsorption efficiency towards dyes. Several surface-modified magnetic nano-adsorbents such as poly (acrylic acid) modified magnetite,[12] sodium dodecyl sulfate modified maghemite,[13] and amino-silane

Correspondence to: N. Hasirci (nhasirci@metu.edu.tr).
Contract grant sponsor: Gazi University; contract grant number: Research Foundation Project No: 05/2009-29.

modified magnetic nanoparticles[14]; magnetic composites based on poly(oxy-2,6-dimethyl-1,4-phenylene)[15] and magnetic multiwall carbon nanotubes,[16] carboxymethyl β-cyclodextrin conjugated magnetic nanoparticles,[17] and magnetic TiO_2 nanoparticles[18] were used for removal of dyes from aqueous media.

Chitosan (CS) is a biopolymer of glucosamine obtained from the deacetylation of chitin and economically attractive polymer.[19] It has high biocompatible, biodegradable, antibacterial, nontoxic, and chelating abilities that make it useful for various biological, biotechnological, and biomedical applications. High chelating capability of CS and its physical versatility of manufacturing (e.g., films, membranes, fibers, sponges, gels, beads, nanoparticles, coatings on inert materials etc.), make it useful for the adsorption and removal of several dyes from discharge waters.[20–23] However, applications of CS modified magnetic nano adsorbents for the removal of dyes are very limited and getting interest especially in the last years.

Reactive dyes are highly water soluble and extensively used in textile industry due to their ability to bind to textile fibers by covalent bonds through their functional groups.[24] There are reports related to the removal of these dyes from wastewaters by using different adsorbents such as, adsorption of Reactive Red 189 onto CS beads,[25] removal of Reactive Black 5 and Reactive Red 31 by activated carbons[26] and adsorption of Reactive Brillant Blue onto polymeric adsorbents,[27] etc.

The main purpose of this study is to prepare CS coated magnetite nanoparticles (Fe_3O_4-CS) as dye adsorbents with a high magnetic property and investigate their adsorption capabilities towards a model azo reactive textile dye, Reactive Yellow 145 (RY145). For this purpose, the prepared Fe_3O_4-CS nanoparticles were first characterized by TEM, XRD, TGA, and EPR, and then the effects of some parameters on the adsorption of RY145 (e.g., dye concentration, pH, temperature and salt concentration) were investigated. Thermodynamics of the adsorption process and desorption of RY145 from the magnetic nano adsorbent were also studied.

MATERIALS AND METHODS

Materials

Fe_3O_4 nanoparticles (<50 nm) was purchased from Aldrich (Steinheim, Germany). CS from crab shells (≥75% deacetylated), acetic acid, and mineral oil were supplied from Sigma (Steinheim, Germany). Ethanol was purchased from Riedel de Haen (Seelze, Germany). Tween 80 was obtained from Acros Organics (NJ, USA). Glutaraldehyde was obtained from British Drug House (Poole, England). RY145 was supplied from Burboya (Bursa, Turkey). All reagents used in this study were analytical grade.

Preparation of chitosan coated magnetite nanoparticles

Coating of Fe_3O_4 nanoparticles with CS were achieved by reversed phase suspension technique after the modification of the procedure given in literature.[28] For this purpose, Fe_3O_4 nanoparticles (200 mg) were dispersed in mineral oil (50.0 mL) containing Tween 80, by ultrasonication. CS solution (1% w/v, 15.0 mL) was added to the medium and the mixture was sonicated for 30 min. The system was stirred with the rate of 1500 rpm and glutaraldehyde solution (3.0 mL, 25% w/v in water) was added. After 4 h stirring at room temperature, the resultant CS coated magnetite nanoparticles (Fe_3O_4-CS) were removed from the reaction mixture with help of a permanent magnet. The obtained nanoparticles were washed several times with acetone and dried in vacuum oven at 40°C.

Characterization of magnetite and chitosan coated magnetite nanoparticles

The particle sizes of Fe_3O_4 and Fe_3O_4-CS nanoparticles were estimated from the images obtained from transmission electron microscope (TEM, Technai^{TM} G^2 F30, Hillsboro, OR) at 100 kV.

The thermal properties of Fe_3O_4 and Fe_3O_4-CS nanoparticles were investigated by a thermogravimetric analyzer (TGA, Perkin–Elmer Pyris 1 TGA, MA). Samples (about 5 mg) were heated from 30 to 700°C at a heating rate of 10 °C min^{-1} in N_2 atmosphere.

The crystal structures of Fe_3O_4 and Fe_3O_4-CS nanoparticles were investigated by X-ray diffractometer (XRD, Rigaku Ultima-IV, Tokyo, Japan) using monochromatized CuKα radiation with 4° min^{-1} scan rate. A continuous scan mode was used to collect 2θ data from 10° to 90°.

Zeta (ζ)-potential of the Fe_3O_4 and Fe_3O_4-CS nanoparticles were measured at 25°C by ζ-sizer (Malvern Nano ZS90, Worcestershire, England) in the range of pH 2.0–9.5. The pH value of the medium was adjusted by using $10^{-2}M$ HCl or NaOH.

For EPR analysis, the Fe_3O_4 and Fe_3O_4-CS nanoparticles (about 40 mg) were placed into quartz tubes and the measurements were carried out with a conventional X-band spectrometer (FT-EPR, Bruker ELEXSYS E 580, Rheinstetten, Germany) at 100 kHz magnetic field modulation frequency, 1 G modulation amplitude and 99 mW microwave power. The first derivative of the power absorption was recorded as a function of the applied magnetic induction.

Adsorption of RY145 onto Fe_3O_4-CS nanoparticles

Effect of contact time

Fe_3O_4-CS nanoparticles (50 mg) were put into a series of flasks containing 25.0 mL of RY145 solution (100 mg L^{-1}; pH 3.0). The mixtures were ultrasonicated for 5 min and replaced into a water bath with shaking rate of 250 cycle min^{-1} at 25°C. At predetermined time intervals, Fe_3O_4-CS nanoparticles were collected with a permanent magnet and the absorbance of the solutions were measured by a UV–visible spectrophotometer (Shimadzu PharmaSpec 1700, Tokyo, Japan) at 419 nm which is maximum absorbance wavelength of the dye. The residual concentration of the dye was determined from the calibration curve of RY145 which was prepared in the range of 0–200 mg L^{-1}. The adsorbed amount of the dye for per gram of nanoparticles (q) was calculated as follows:

$$q = [(C_i - C_f) \times V]/W \quad (1)$$

where q represents the amount of dye adsorbed (mg g^{-1}), C_i and C_f are the initial and final concentrations of RY145 (mg L^{-1}), V is the volume of the solution (L) and W is the weight (g) of Fe_3O_4-CS nanoparticles.

Effect of pH

Effect of pH on the adsorption of RY145 on Fe_3O_4-CS nanoparticles was investigated between pH 3.0 and 11.0. For this purpose, Fe_3O_4-CS nanoparticles (50 mg) were placed into flasks, RY145 solutions (25.0 mL having 100 mg L^{-1}; at pH 3.0, 4.0, 5.0, 6.0, 7.0, 8.0, 9.0, 10.0, and 11.0) were added and the mixtures were sonicated for 5 min. After keeping the mixtures at 25°C for 90 min, nanoparticles were collected with a permanent magnet. The absorbance values of the solutions were obtained at 419 nm and the residual concentration of the dye was determined as described above.

Adsorption isotherms and effect of temperature

Adsorption isotherms of RY145 on Fe_3O_4-CS nanoparticles were obtained in the temperature range of 25–45°C. For this purpose, nanoparticles (50 mg) were placed into flasks containing RY145 solutions (25.0 mL) with different concentrations (50.0, 75.0, 100.0, 125.0, 150.0, 175.0, and 200 mg L^{-1}) at pH 3.0, and the mixtures were sonicated for 5 min. The systems were placed in a shaking water bath at constant temperatures of 25°C, 35°C, and 45°C. Fe_3O_4-CS nanoparticles were collected with a permanent magnet after 90 min, and residual concentration of the dye was determined as described above.

Effect of salt concentration

The effect of salt concentration on the adsorption of RY145 on Fe_3O_4-CS nanoparticles was investigated in the medium containing KCl in the range of 10.0–50.0 m*M*. As described above, the RY145 solutions (100 mg L^{-1}, pH 3.0) were prepared and KCl were added to form a final concentration in the range of 10.0, 20.0, 30.0, 40.0, 50.0 m*M*. The solutions were mixed with Fe_3O_4-CS nanoparticles (50 mg). The mixtures were sonicated for 5 min at 25°C. After 90 min, magnetic nanoparticles were removed with a permanent magnet and the absorbances of the dye solutions were determined.

Desorption studies

For desorption experiments, dye loaded Fe_3O_4-CS nanoparticles were prepared as follows: 25.0 mL RY145 solutions (100 mg L^{-1}; pH 3.0) were mixed with Fe_3O_4-CS nanoparticles (50 mg) and the mixtures were sonicated for 5 min. The systems were placed in a shaking water bath with stirring rate of 250 cycle min^{-1} at 25°C. After 90 min, dye loaded Fe_3O_4-CS nanoparticles were collected with a permanent magnet and dye solutions were removed. Dye loaded Fe_3O_4-CS nanoparticles were mixed with NaOH solution (25.0 mL with concentrations of 2.5, 5.0, 7.5, and 10.0 m*M*) and the flasks were agitated for 90 min at 25°C. The amounts of the dye desorbed from the nanoparticles were found from the absorbance values of the solutions.

RESULTS AND DISCUSSION

Characterization of Fe_3O_4-CS nanoparticles

The particle size of the magnetic Fe_3O_4-CS nanoparticles and the thickness of the CS coating were estimated from TEM images (Fig. 1). The diameters of the uncoated Fe_3O_4 nanoparticles were less than 50 nm [Fig. 1(a)]. It was observed that the CS layer completely covered the surface of the Fe_3O_4 nanoparticles [Fig. 1(b)] and the thickness of CS layer was estimated as 1.8–4.8 nm by using Image J program.

The XRD patterns of Fe_3O_4 and Fe_3O_4-CS nanoparticles are shown in Figure 2. For Fe_3O_4, six peaks (2θ = 30.18°, 35.47°, 43.30°, 53.42°, 57.18°, and 62.70°) were detected and it was observed that these peaks coincide with those of the JCPDS card (65-3107) given for Fe_3O_4. On the other hand, the same six characteristic peaks were also detected for Fe_3O_4-CS nanoparticles, showing that magnetite retained its form with the same spinel structure as same as pure Fe_3O_4. It is concluded that the coating process did not show any phase change of Fe_3O_4.

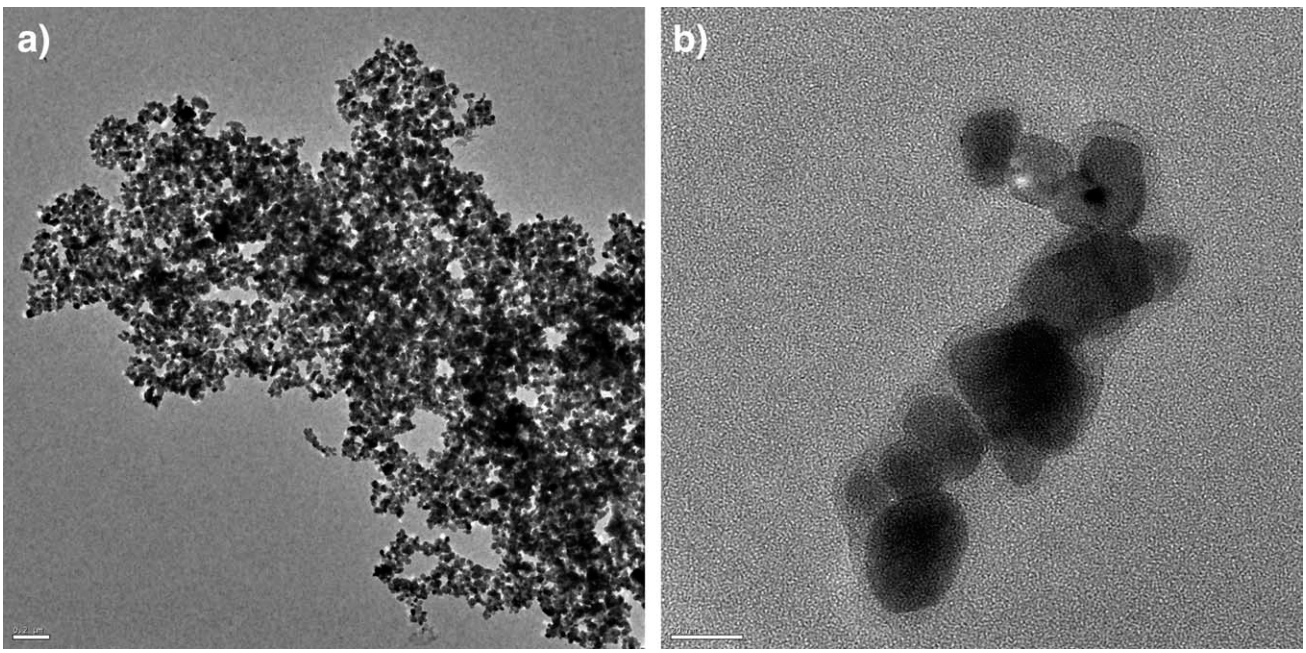

Figure 1 TEM images of Fe_3O_4 (a) and Fe_3O_4-CS (b) nanoparticles (Scales: (a) 0.2 μm, (b) 20 nm).

The crystallite size can be estimated by X-ray powder diffraction patterns from the measurement of the half-height width of the strongest reflection plane by using Debye–Scherrer formula as follows:

$$d = (k\lambda/\beta\cos\theta) \quad (2)$$

In this equation, d is the thickness of the crystal, k is the Debye–Scherrer constant (0.89), λ is the X-ray wavelength (0.15406 nm) and β is the line broadening in radian obtained from the full width at half maximum, θ is the Bragg angle.[18] β and θ values for the strongest reflection plane of XRD patterns were found to be 9.07×10^{-3} and 17.73 for Fe_3O_4 and 8.20×10^{-3} and 17.72 for Fe_3O_4-CS, respectively. From eq. (2), the average diameters of Fe_3O_4 and Fe_3O_4-CS were calculated as 16 nm and 18 nm, respectively. It was observed that these results are in accordance with the size of the particles determined by TEM.

The CS content of Fe_3O_4-CS nanoparticles was estimated from TGA (Fig. 3). The weight loss of Fe_3O_4 nanoparticles was about 1% between 30°C and 700°C [Fig. 3(a)]. This might be due to the loss of residual water from the sample. For Fe_3O_4-CS nanoparticles, the weight loss was about 5.7% below 200°C similarly because of the removal of absorbed water by physical and chemical attractions,[28] but the significant degradation at 200–550°C corresponds to the breakdown of the main CS chains covering the magnetic nanoparticles. There was no significant change after 550°C, implying the presence of iron oxide above this temperature. For CS, an initial loss

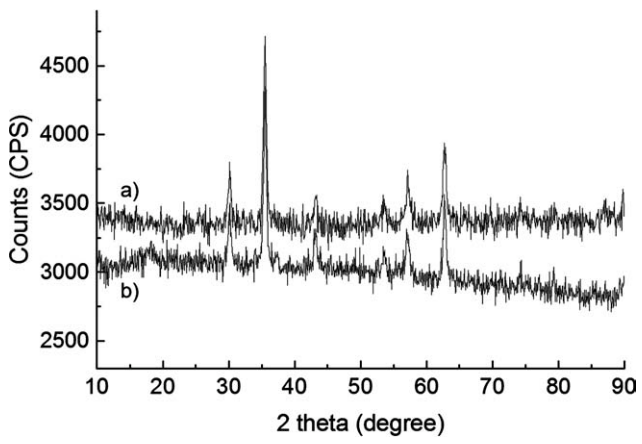

Figure 2 XRD patterns of Fe_3O_4 (a) and Fe_3O_4-CS (b) nanoparticles.

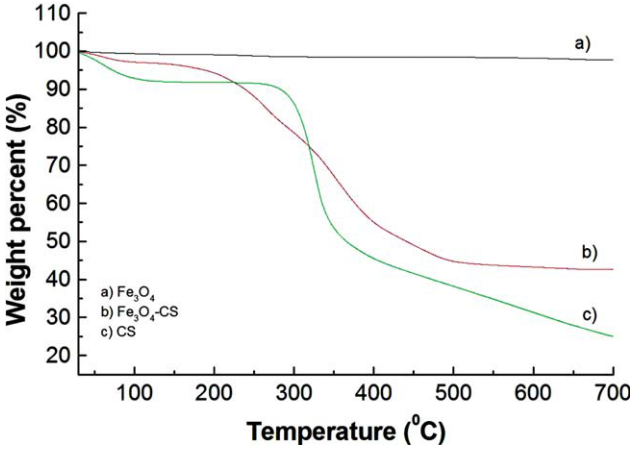

Figure 3 TGA thermograms of Fe_3O_4 (a) and Fe_3O_4-CS (b) nanoparticles, and pure CS powder (c).

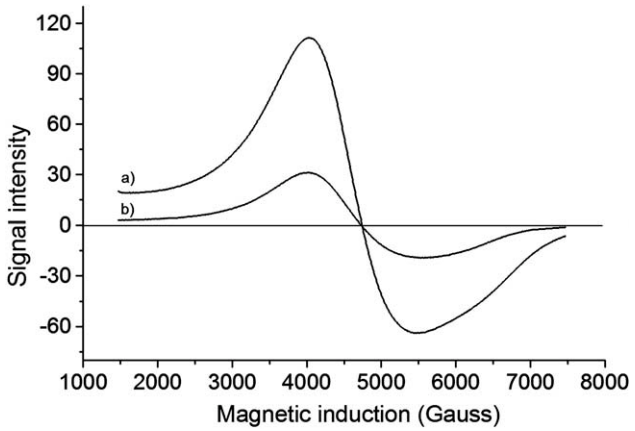

Figure 4 EPR spectra of Fe_3O_4 (a) and Fe_3O_4-CS (b) nanoparticles.

of water (about 8%) was observed below 200°C, followed by decomposition of its acetylated and deacetylated units occurring at 300–400°C. In fact, the thermal decomposition of pure CS continues even after 700°C [Fig. 3(c)], most probably due to the strong interactions among macromolecules and presence of crystal domains. But for Fe_3O_4-CS nanoparticles [Fig. 3(b)], the morphology and crosslinked organization of CS chains are different than pure CS structure and it seems that all of it degrades below 500°C. Based on the thermograms, the CS content of Fe_3O_4-CS nanoparticles was estimated about 50% [Fig. 3(b)].

EPR spectra of Fe_3O_4 and Fe_3O_4-CS nanoparticles are presented in Figure 4. For Fe_3O_4-CS nanoparticles, signal intensity related to the absorption of the applied magnetic field is lower than the uncoated nanoparticles. The total effective magnetic moment of the samples decreased due to the CS coating. Noncollinear spin structure originated from the pinning of the surface spins and coated surfactant at the interface of nanoparticles causes this decrease. The contribution of the volume of the diamagnetic coating mass to the total sample volume can be another reason of this effect.[29] For both samples, resonance magnetic field (B_0) was determined as 4735 G, and spectroscopic g factor was calculated as 1.49. In the literature, the g factor of Fe^{3+} was reported in the ranges of 1.4–3.1 for low spin complexes and 2.0–9.7 for high spin complexes.[30] Therefore, it can be concluded that Fe_3O_4 and Fe_3O_4-CS nanoparticles used in this study are in the state of low-spin Fe^{3+} complex.

Adsorption of RY145 onto Fe_3O_4-CS nanoparticles

Effect of contact time

The effect of contact time on the adsorption of RY145 onto Fe_3O_4-CS nanoparticles (at 25°C, pH 3.0, the initial dye concentration = C_0 = 100 mg L^{-1}) is given in Figure 5. The adsorption of RY145 increased within the first 60 min and then equilibrated at about 90 min. Therefore, the experiments were carried out for 90 min.

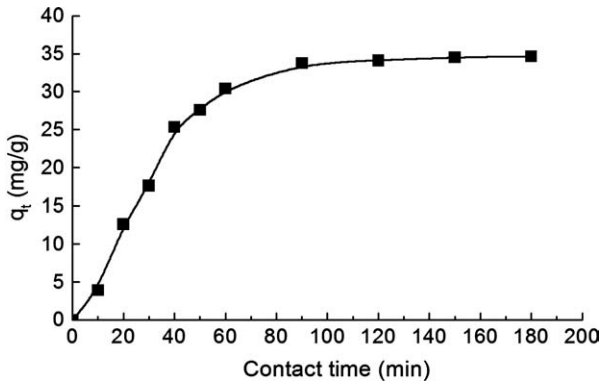

Figure 5 Effect of contact time on the adsorption of RY145 onto Fe_3O_4-CS nanoparticles. (C_o = 100 mg L^{-1}, 50 mg Fe_3O_4-CS, V_{Total} = 25.0 mL, pH = 3.0, 25°C).

The equilibrium time of the adsorption depends on the adsorbed molecules and the properties of the adsorbent. There are reports showing the adsorption equilibrium times were 20–30 min for Acid Orange 12 and Acid Green 25 collected on carboxymethylated CS-conjugated magnetic nanoparticles,[11] 60 min for Acid Orange 10 collected on magnetic silica particles,[14] 60–90 min for azo, triarylmethane, and polycyclic dyes collected on magnetic poly(oxi-2,6-dimethyl-1,4-phenyl) composites.[15] Therefore the value of 90 min applied in this study is in accordance with the literature values.

Effect of pH

The effect of pH on the adsorption of RY145 onto Fe_3O_4-CS nanoparticles at 25°C is shown in Figure 6. The maximum adsorption was obtained at pH 3.0, q_e values were almost constant in the pH range 3.0–5.0

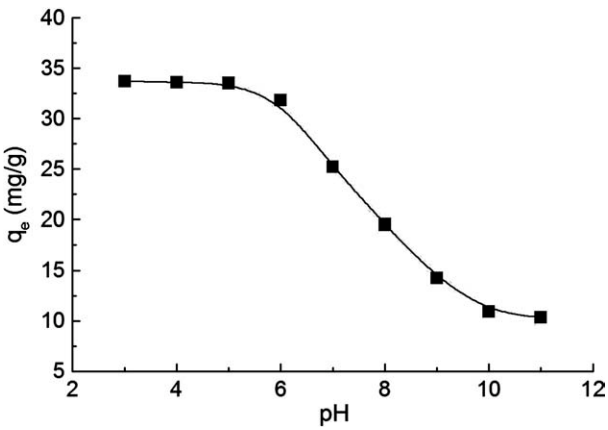

Figure 6 Effect of pH on the adsorption of RY145 onto Fe_3O_4-CS nanoparticles. (C_o = 100 mg L^{-1}, 50 mg Fe_3O_4-CS, V_{Total} = 25.0 mL, 25°C).

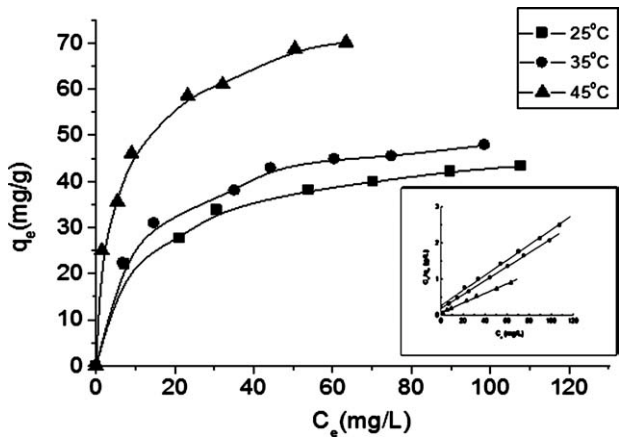

Figure 7 Adsorption isotherms for adsorption of RY145 onto Fe_3O_4-CS nanoparticles. Inset: fitted by Langmuir adsorption model. (C_o = 50–200 mg L^{-1}, 50 mg Fe_3O_4-CS, V_{Total} = 25.0 mL, pH = 3.0, 25°C, 35°C, and 45°C).

and a decrease was observed after pH 5.0. Fe_3O_4-CS nanoparticles had the highest ζ-potential value (24 mV) at about pH 3.0 (data not shown). The isoelectric point (pI) is the pH value where ζ-potential is equal to zero and this point is also defined as "zero point charge" (pH_{zpc}) at which there is no net adsorption of proton or hydroxide ions. In water, where there are no added electrolytes, these values are equal to each other, and found as 6.86 for Fe_3O_4-CS nanoparticles. pI values reveal that at acidic pH conditions positive charge is dominated on the surface of these nanoparticles. This phenomenon was consistent with the pH-dependence of ζ-potential and could be attributed to the increased electrostatic attractions between the negatively charged sulfonate groups ($-SO_3^-$) of RY145 dye and the positively charged protonated amine groups of CS at lower pH values. In addition, the adsorption capacity of the particles was decreased significantly above pH 7.0. At high pH, protonation of the CS's amino group would not take place (p*Ka*∼ 6.5) Therefore, due to the repulsions of the negative charges existing on both adsorbent and the dye will cause a decrease in the adsorption.

Effect of temperature

Adsorption data carried out at various temperatures can be used to obtain adsorption isotherms which are important in design of the adsorption system to remove the dye.

Langmuir model has the assumptions that adsorption takes place at specific sites which are identical and energetically equal to each other; once a molecule is adsorbed on the site it has no positive or negative effect on the adsorption of the neighboring sites, the adsorption is monolayer and reach to equilibrium after all sites are occupied. On the other hand, Freundlich model has the assumptions that the adsorbent has heterogeneous sites, adsorption energy exponentially decreases on completion of the adsorptive sites adsorption, and the adsorption is multilayer.

The adsorption isotherms of RY145 onto Fe_3O_4-CS nanoparticles at different temperatures are given in Figure 7. The equations for Langmuir [eq. (3)] and Freundlich [eq. (4)] models are given below:

$$C_e/q_e = 1/K_L q_{max} + C_e/q_{max} \quad (3)$$

$$q_e = K_F C_e^{1/n} \quad (4)$$

where, C_e is the equilibrium concentration of dyes in solution (mg L^{-1}), q_e is the adsorbed amount of dyes at equilibrium concentration (mg g^{-1}), q_{max} is the maximum adsorption capacity (mg g^{-1}), and K_L is the Langmuir binding constant which is related to the energy of adsorption (L mg^{-1}), K_F (L g^{-1}) and n are the Freundlich constants related to the adsorption capacity and intensity, respectively.[14,20] Plotting C_e/q_e against C_e gives a straight line with slope and intercept equal to $1/q_{max}$ and $1/K_L q_{max}$, respectively, (inserted in graph Fig. 7).

Langmuir and Freundlich constants at different temperatures for adsorption of RY145 were calculated and reported in Table I. It was observed that, the values of q_{max} obtained from Langmuir plots at different temperatures are mainly consistent with the experimentally obtained values. It can be concluded that the adsorption process is mainly monolayer. According to the r^2 values reported in Table I, experimental data of adsorption better fits to Langmuir model than Freundlich model, indicating the homogeneity of active sites on the surface of Fe_3O_4-CS nanoparticles.

The essential features of Langmuir adsorption isotherm can be expressed in terms of a dimensionless

TABLE I
Langmuir and Freundlich Constants for Adsorption of RY145 onto Fe3O4-CS Nanoparticles

	Langmuir constants					Freudlich constants		
Temperature (°C)	$q_{max,\ calc}$ (mg g^{-1})	$q_{max,\ exp}$ (mg g^{-1})	K_L (L mg^{-1})	R_L	r^2	n	K_F (L g^{-1})	r^2
25	47.62	43.30	0.0789	0.20–0.06	0.996	3.788	12.94	0.987
35	52.63	47.83	0.1016	0.16–0.05	0.999	3.546	14.00	0.947
45	76.92	70.10	0.1806	0.10–0.03	0.995	3.557	23.01	0.985

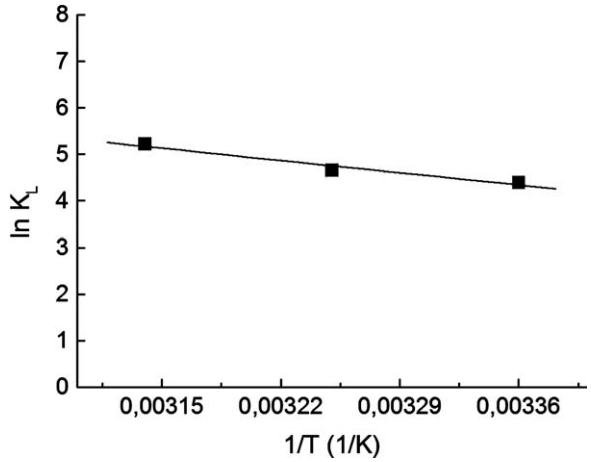

Figure 8 van't Hoff plot for the adsorption of RY145 onto Fe_3O_4-CS nanoparticles. (C_o = 50–200 mg L^{-1}, 50 mg Fe_3O_4-CS, V_{Total} = 25.0 mL, pH = 3.0, 25°C, 35°C, and 45°C).

constant called separation factor or equilibrium parameter (R_L), which is defined by the following relationship[14]:

$$R_L = 1/(1 + K_L C_o) \quad (5)$$

where C_o is the initial concentration of dye (mg L^{-1}). The value of R_L indicates the nature of adsorption isotherm where $0 < R_L < 1$ shows favorability of the process, $R_L = 1$ and $R_L = 0$ defines unfavorable and irreversible processes, respectively. As shown in Table I, the calculated values of R_L were found in between 0 and 1. This implies that the adsorption of RY145 on Fe_3O_4-CS nanoparticles from aqueous solutions is favorable under the given conditions.

The thermodynamics of adsorption can be investigated by the values of K_L at different temperatures according to the following van't Hoff equation[20]:

$$\ln K_L = -\Delta H^o/RT + \Delta S^o/R \quad (6)$$

In this equation, ΔH^o and ΔS^o are enthalpy and entropy changes of adsorption process, respectively, R is the universal gas constant (8.314 J mol^{-1} K^{-1}) and T is the absolute temperature (K). Plotting ln K_L against $1/T$ (Fig. 8) gives a straight line with slope and intercept equal to $-\Delta H^o/R$ and $\Delta S^o/R$, respectively. From this figure, ΔH° and ΔS° values were calculated as 31.37 kJ mol^{-1} and 141.46 J mol^{-1} K^{-1}, respectively.

The positive value of ΔH° indicates that the adsorption process is endothermic. For simple adsorption process, the interaction between adsorptive support and adsorbent molecules elaborates that heat and the enthalpy change is negative. Also, adsorbed dye molecules become more ordered position causing a decrease in entropy. But, for hydrophilic polymers with partially charged domains in their structure, the reverse observations can be obtained.[20] For these materials, water molecules form a hydrated shell having strong interactions and hydrogen bonds with the polymeric layer. In some cases these water molecules are strongly linked to the surface that they may called as "ice like water" molecules. In these cases, adsorption of the dye increases as temperature increases, since the given heat destroys this water shielding around the particles and opens the sites for dye molecules. In this work, the heat needed to break this hydrated shell is higher than the heat released by dye adsorption. Therefore, positive enthalpy change was obtained. On the other hand, the positive value of ΔS° for the adsorption shows an increase of the randomness during the adsorption of RY145. This might be due to the liberation of water molecules from the hydrated shells of the adsorbed species.[20,31]

TABLE II
$\Delta G°$ vs. $T\Delta S°$ Values at Different Temperatures for the Adsorption of RY145 onto Fe3O4-CS Nanoparticles

Temperature (K)	ΔG° (kJ mol^{-1})	$T\Delta S^\circ$ (kJ mol^{-1})
298	−10.79	42.16
308	−12.20	43.57
318	−13.61	44.98

Gibbs free energy of the adsorption (ΔG^o) can be calculated from the following equation and given in Table II.

$$\Delta G^o = \Delta H^o - T\Delta S^o \quad (7)$$

ΔG^o value of the adsorption at 25°C was found to be −10.79 kJ mol^{-1}. The negative value of ΔG^o shows spontaneity of adsorption process, and increase in negative values parallel to temperature indicates favorability of the adsorption at higher temperatures. On the other hand, positive value of

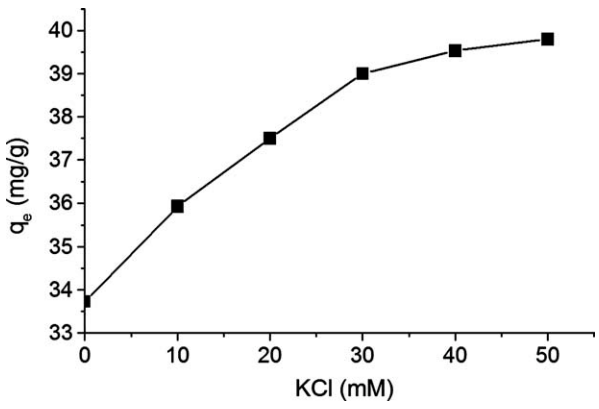

Figure 9 The effect of KCl concentration on the adsorption of RY145 onto Fe_3O_4-CS nanoparticles. (C_o = 100 mg L^{-1}, 50 mg Fe_3O_4-CS, V_{Total} = 25.0 mL, 25°C).

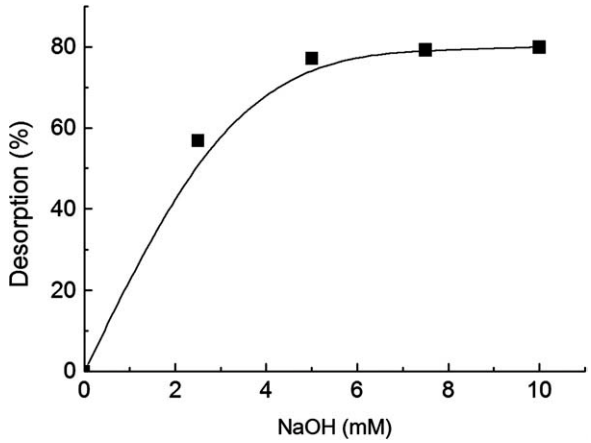

Figure 10 Desorption of RY145 from Fe_3O_4-CS nanoparticles at different NaOH concentrations. (50 mg Fe_3O_4-CS, $V_{Total} = 25.0$ mL, 25°C).

entropy is the result of dehydration and this cause an increase in K_L values as temperature increases. Since, entropy has positive value, it is concluded that entropic changes are dominant in the adsorption process.

Effect of salt concentration

The effect of KCl concentration on the adsorption of RY145 onto Fe_3O_4-CS nanoparticles was investigated for various KCl concentrations in the range of 0–50.0 m*M* at 25°C. Adsorbed amount of dye at equilibrium concentration (q_e) versus KCl concentration were plotted (Fig. 9). The values of q_e increased from 33.73 mg g^{-1} to 39.80 mg g^{-1} as the KCl concentration increased from 0 to 50.0 m*M*. Presence of KCl in the adsorption medium causes formation of an electrical double layer around the nanoparticles. In this case, negatively charged Cl^- ions diffuse to the CS particle surface and try to equilibrate the surface charge. Positively charged K^+ ions also diffuse to the surface and form the second layer. The thickness of electrical double layer depends on the concentration and charge. As the concentration of the electrolyte increases, the counter ions get closer to the surface and the thickness of the electrical double layer decreases. This leads higher adsorption in Stern layer.[32]

Desorption of dye from the adsorbent

Desorption of RY145 from Fe_3O_4-CS nanoparticles was carried out by using 2.5–10.0 m*M* NaOH solutions and expressed as percentage of the totally adsorbed RY145 (Fig. 10). The results showed that desorption percentage of RY145 increased as the concentration of NaOH increased and about 80% of the adsorbed RY145 was desorbed by using 10.0 m*M* NaOH over one adsorption/desorption cycle. This can be explained by the decrease of the electrostatic interactions between Fe_3O_4-CS nanoparticles and RY145 molecules as the concentration of NaOH increased and pH of the medium shifted to higher values. Similar trend was reported in literature for desorption of Acid Orange 10 from modified magnetic silica particles as the pH of the desorption media increased from 7.0 to 10.0.[14]

CONCLUSIONS

The CS coated magnetic nanoparticles (Fe_3O_4-CS) were prepared and their efficiency as a magnetic nano-adsorbent against a reactive azo textile dye, RY145, was investigated first time in literature. It was found that the adsorption capacities of RY145 increased by increasing the temperature in the range of 25–45°C and concentration of KCl up to 50.0 m*M*; and decreased with increasing pH of the adsorption medium in the pH range of 3.0–11.0. These results revealed that the prepared nanoparticles exhibit very efficient adsorption for the removal of azo dyes when the parameters of the medium are $T = 25$–45°C, pH = 3.0–5.0 and salt concentration = 30–50 m*M*. Moreover, the prepared magnetic nanoparticles can be easily separated from the media with a help of a magnet which makes those nanoparticles more advantageous compared to nonmagnetic nanoadsorbents. Desorption of the adsorbed dye can be achieved easily by NaOH treatment and about 80% of the adsorbed dye can be desorbed over one cycle, revealing that these nanoparticles can be used repeatedly after regeneration. Therefore, it can be concluded that the prepared magnetically separable CS coated magnetic nano-adsorbents with a high adsorption capacity can be good candidates for removal of the dyes from the wastewaters of fabric and textile industries.

Authors thank UNAM, Institute of Materials Science and Nanotechnology, for TEM images; Middle East Technical University, Central Laboratory for other characterization tests.

References

1. Sun, Q. Y.; Yang, L. Z. Water Res 2003, 37, 1535.
2. Kamari, A.; Wan Saime, W. N.; Lai Ken, L. J Environ Sci (China) 2009, 21, 296.
3. Teh, M. C.,Mohamed, A. R. J Alloys Compd 2011, 509, 1648.
4. Gupta Suhas, V. K. J Environ Manage 2009, 90, 2313.
5. Adak, A.; Bandyopadhyay, M.; Pal, A. Sep Purif Technol 2005, 44, 139.
6. Wouters, I.; Quintens, I.; Roets, E.; Hoogmartens, J. J Liq Chromatogr Relat Technol 1990, 13, 253.
7. Ozdemir, O.; Armagan, B.; Turan, M.; Celik, M. S. Dyes Pigm 2004, 62, 49.
8. Pereira, M. F. R.; Soares, S. F.; Órfão, J. J. M.; Figueiredo, J. L. Carbon 2003, 41, 811.

9. Dyal, A.; Loos, K.; Noto, M.; Chang, S. W.; Spagnoli, C.; Shafi, K. V. P. M.; Ulman, A.; Cowman, M.; Gross, R. A. J Am Chem Soc 2003, 125, 1684.
10. Liao, M. H.; Chen, D. H. J Mater Chem 2002, 12, 3654.
11. Chang, Y.-C.; Chen, D.-H. Macromol Biosci 2005, 5, 254.
12. Mak, S.-Y.; Chen, D.-H. Dyes Pigm 2004, 61, 93.
13. Afkhami, A.; Saber-Tehrani, M.; Bagheri, H. Desalination 2010, 263, 240.
14. Atia, A. A.; Donia, A. M.; Al-Amrani, W. A. Chem Eng J 2009, 150, 55.
15. Safarik, I.; Safarikova, M.; Buricova, V. Collect Czech Chem Commun 1995, 60, 1448.
16. Gong, J. L.; Wang, B.; Zeng, G.-M.; Yang, C.-P.; Niu, C.-G.; Niu, Q.-Y.; Zhou, W.-J.; Liang. Y. J Hazard Mater 2009, 164, 1517.
17. Badruddoza, A. Z. M.; Hazel, G. S. S.; Hidajat, K.; Uddin, M. S. Colloid Surface A 2010, 367, 85.
18. Álvarez, P. M.; Jaramillo, J.; López-Pinero, F.; Plucinski, P. K. Appl Catal B Environ 2010, 100, 338.
19. dos Anjos, F. S. C.; Vieira, E. F. S.; Cestari, A. R. J Colloid Interface Sci 2002, 253, 243.
20. Elwakeel, K. Z. J Hazard Mater 2009, 167, 383.
21. Crini, G.; Badot, P.-M. Prog Polym Sci 2008, 33, 399.
22. Qin, Y.; Cai, L.; Feng, D.; Shi, B.; Liu, J.; Zhang, W.; Shen, Y. J Appl Polym Sci 2007, 104, 3581.
23. Wang, S.; Yu, D.; Huang, Y.; Guo, J. J Appl Polym Sci 2065 2011, 119.
24. Zollinger, H. Color Chemistry: Syntheses, Properties and Applications of Organic Dyes and Pigments, 2nd ed.; VCH Publishers: Weinheim, 1991.
25. Chiou, M. S.; Li, H. Y. Chemosphere 2003, 50, 1095.
26. Tanthapanichakoon, W.; Ariyadejwanich, P.; Japthong, P.; Nakagawa, K.; Mukai, S. R.; Tamon, H. Water Res 2005, 39, 1347.
27. Chao, L.; Zhaoyang, L.; Aimin, L.; Wei, L.; Zhenmao, J.; Jinlong, C.; Quanxing, Z. Sep Purif Technol 2005, 44, 115.
28. Li, G.; Jiang, Y.; Huang, K.; Ding, P.; Chen, J. J Alloys Compd 2008, 466, 451.
29. Köseoğlu, Y. J Magn Magn Mater 2006, 300, 327.
30. Swartz, H. M.; Bolton, J. R.; Borg, D. C. Biological Applications of Electron Spin Resonance; Wiley: New York, 1972.
31. Alkan, M.; Demirbaş, Ö.; Çelikçapa, S.; Doğan, M. J Hazard Mater B 2004, 116, 134.
32. Baskaralingam, P.; Pulikesi, M.; Ramamurthi, V.; Sivanesan, S. Appl Clay Sci 2007, 37, 207.